

Scalar field dark energy models with a dynamical equation of state for matter

Koyel Ganguly^{1*}, Sumit Som², and Amitava Sil³

¹Institute of Engineering & Management, School of University of Engineering and Management, Kolkata-700091, India

²Meghnad Saha Institute of Technology, Nazirabad, Kolkata-700150, India

³St. Paul's C. M. College, 33/1 Raja Rammohan Sarani, Kolkata-700009, India

Abstract. The red-shift z_{eq} , which signifies the termination of the radiation-dominated epoch and the onset of the matter-dominated era, can serve as an important diagnostic tool in reconstructing dark-energy models. In this work, we introduce a variable equation of state for matter that enables a smooth and continuous transition from radiation domination to matter domination within a single framework. This formulation allows estimation of z_{eq} in dark energy models and thereby facilitates assessment of their viability. To illustrate this approach, two one-parameter models involving minimally coupled scalar fields as dark energy are examined. We find that, although these models successfully reproduce the desired late-time cosmic behavior, the estimated value of z_{eq} exhibits strong sensitivity to the parameter value in each case.

1 Introduction

Independent observational probes—including type Ia Supernovae (SN Ia) [1], Cosmic Microwave Background radiation (CMBR) [2], and Baryon Acoustic Oscillations [3]—have firmly established that nearly 70% of the present energy density of the universe is contributed by ‘Dark Energy’. Unlike ordinary matter, dark energy exerts a repulsive gravitational effect, and its dominance explains the presently observed accelerated expansion of the universe. Consequently, a major focus of cosmological research over the past decade has been to uncover the origin and physical nature of dark energy.

The most straightforward and natural candidate for dark energy is the Cosmological Constant Λ , characterized by the equation of state $\omega_{DE} = -1$. However, if vacuum energy is regarded as its origin, theoretical estimates overshoot observationally required values by nearly 120 orders of magnitude. Attempts to reconcile this discrepancy include models with a varying Λ while retaining $\omega_{DE} = -1$ [4]. Models featuring an evolving ω_{DE} have also been widely explored in dynamical dark energy scenarios. Prominent examples include scalar field constructions such as Quintessence [5] and K-essence [6]. Despite their flexibility in accommodating evolving ω_{DE} and matching observational features, these models do not necessarily provide decisive advantages over the Λ Cold-Dark-Matter (Λ CDM)

*Corresponding Author:koyel.ganguly@iem.edu.in

model. Furthermore, generating late-time acceleration often requires extremely flat potentials, implying exceedingly small scalar field masses [7]. Nevertheless, scalar field dark energy models remain theoretically appealing within particle physics and cannot be excluded. Other dynamical dark energy candidates include modified matter models such as Chaplygin gas [8], as well as modified gravity theories like $f(R)$ gravity [9], Scalar-Tensor theories [10], and Braneworld scenarios [11]. Comprehensive reviews of dark energy may be consulted for further details [12].

In most existing studies, such models are analyzed primarily during the matter-dominated era, assuming dark energy drives the transition from deceleration to acceleration. This emphasis arises because the radiation epoch was brief and confined to the early universe, whereas acceleration is a comparatively recent phenomenon within the matter-dominated epoch. Viability is typically assessed by comparing theoretical predictions—such as the evolution of the deceleration parameter q with redshift z —against observational data. While the transition redshift z_t (marking deceleration to acceleration) is well constrained, observations span only a limited redshift range near z_t . Consequently, models consistent within this range may diverge substantially outside it. To discriminate among such models, an additional well-constrained event from an earlier epoch is desirable. We emphasize that a reliable estimate of z_{eq} —the redshift at matter–radiation equality—is available. Thus, instead of a single observational anchor point, we obtain two widely separated constraints through which any viable q versus z trajectory must pass. A model satisfying both constraints is more robust across cosmic history. However, estimating z_{eq} necessitates a framework containing both radiation and matter simultaneously. In earlier work [13], we introduced a variable equation of state that reproduces radiation behavior in the early universe and pressureless dust at later times. We also demonstrated how this approach helps select among competing varying Λ models.

In the following section, we restate the proposed variable equation of state for completeness. Subsequently, two scalar field models incorporating this equation of state are analyzed to illustrate the method.

2 Radiation and matter in a single model

We consider a flat Robertson-Walker spacetime motivated by strong observational support for spatial flatness [14]. In Friedmann cosmology, such a homogeneous and isotropic universe is filled with an ideal fluid whose equation of state is either that of radiation ($p_r = \frac{1}{3}\rho_r$) or pressureless dust ($p_m = 0$). In the standard cosmological picture without dark energy, radiation dominates during approximately the first 2000 years of cosmic evolution, followed by matter domination. Traditionally, this requires stitching together two distinct cosmological phases with different equations of state.

Earlier attempts to describe the entire evolution within a single framework were undertaken by Chernin [15], McIntosh [16], Landsberg and Park [17], Jacobs [18], and Cohen [19]. In those approaches, the universe contains two non-interacting components: radiation and matter. Radiation energy density evolves as $\rho_r \sim a^{-4}$, while matter evolves as $\rho_m \sim a^{-3}$. Hence the total density and pressure are

$$\rho = \rho_{r0}(a_0/a)^4 + \rho_{m0}(a_0/a)^3 \quad (1)$$

$$p = \frac{1}{3}\rho_{r0}(a_0/a)^4 \quad (2)$$

This yields the effective equation of state

$$f = \frac{p}{\rho} = \frac{1}{3} [1 + (\rho_{m0}/\rho_{r0})(a/a_0)]^{-1} = \frac{1}{3} \left[1 + \frac{a}{a_{eq}} \right]^{-1} \quad (3)$$

For $a \ll a_{eq}$, the behavior approaches pure radiation; for $a \gg a_{eq}$, pressure becomes negligible, reproducing matter domination.

We adopt this equation of state for the cosmological fluid. In the presence of dark energy, this unified treatment allows simultaneous assessment of both z_{eq} and z_t . As shown previously [13], this

improves discrimination among models. In this work, we apply the method to scalar field dark energy models.

3 Field Equations

For a homogeneous and isotropic flat Robertson-Walker spacetime described by the metric

$$ds^2 = -dt^2 + a^2(dr^2 + r^2 d\theta^2 + r^2 \sin^2 \theta d\phi^2) \quad (4)$$

the Einstein field equations corresponding to a two-component cosmic fluid take the form

$$\begin{aligned} 3H^2 &= \rho + \rho_\phi & (5) \\ \text{and} \quad 2\dot{H} + 3H^2 &= -(p + p_\phi) & (6) \end{aligned}$$

where an overdot denotes differentiation with respect to cosmic time. Here ρ and p represent the energy density and pressure of the background cosmological fluid, whereas ρ_ϕ and p_ϕ denote the corresponding quantities for the dark energy component. Throughout this paper, the suffix ϕ refers exclusively to the dark energy contribution. The Hubble parameter is defined in the usual manner as $H \equiv \dot{a}/a$.

These field equations may equivalently be expressed in terms of density parameters and equations of state as

$$\begin{aligned} 1 &= \Omega + \Omega_\phi & (7) \\ \text{and} \quad \frac{1}{3}(2q - 1) &= \omega\Omega + \omega_\phi\Omega_\phi & (8) \end{aligned}$$

where the deceleration parameter q , equation of state parameter ω , and density parameter Ω are defined conventionally by

$$\begin{aligned} q &\equiv -\ddot{a}/aH^2 \\ \omega &\equiv p/\rho \\ \text{and} \quad \Omega &\equiv \rho/3H^2. \end{aligned}$$

If dark energy is modeled as a minimally coupled scalar field, one may begin with the action

$$\mathcal{A} = \int d^4x \sqrt{-g} \left[\frac{R}{16\pi G} + \frac{1}{2} \phi_{,\mu} \phi^{,\mu} - V(\phi) + \mathcal{L} \right] \quad (9)$$

which reproduces the field equations (5) and (6) with

$$\begin{aligned} \rho_\phi &= \frac{1}{2} \dot{\phi}^2 + V(\phi) & (10) \\ \text{and} \quad p_\phi &= \frac{1}{2} \dot{\phi}^2 - V(\phi). & (11) \end{aligned}$$

Altogether, there are five unknown quantities, namely H , ϕ , $V(\phi)$, ρ , and p . Since only two independent field equations are available, three additional assumptions are required for closure.

1. For late-time evolution, the background matter may be approximated as pressureless dust, so $p = p_m = 0$. This assumption is adopted in Model 1 and Model 2. In contrast, Models 1A and 2A incorporate radiation, and therefore $p \neq 0$ in those cases.

2. We assume that there is no interaction between the background fluid and the dark energy component. Consequently, the conservation equation

$$\dot{\rho} + 3H(\rho + p) = 0 \quad (12)$$

holds, along with the scalar field wave equation

$$\ddot{\phi} + 3H\dot{\phi} + V'(\phi) = 0 \quad (13)$$

where a prime denotes differentiation with respect to ϕ .

3. Finally, we impose a specific constraint on the behavior of the scalar field to ensure late-time acceleration. Two different choices are considered. The first is implemented in Model 1 and Model 1A, while the second is employed in Model 2 and Model 2A.

4 Model 1

In this model the background matter is taken to be dust, so $p = 0$. The conservation equation (12) then directly yields

$$\rho = R_1 a^{-3}. \quad (14)$$

The scalar field is assumed to evolve as

$$\phi = \beta \ln a. \quad (15)$$

This assumption resembles the common choice $\phi = \alpha \ln t$ used in power-law expansion models that generate exponential-type potentials.

Using (14), the field equations may be solved to obtain

$$V(\phi) = \frac{R_1 \beta^2}{2(3 - \beta^2)} e^{-\frac{3}{\beta}\phi} + C_1 e^{-\beta\phi}. \quad (16)$$

Exponential potentials are well known in the literature for producing accelerated expansion in scalar field dark energy models[20].

If a_t denotes the scale factor at which the universe transitions from deceleration to acceleration, then q must vanish at $a = a_t$. Imposing this condition determines the integration constant C_1 as

$$C_1 = \frac{R_1(6 - \beta^2)}{2(3 - \beta^2)(2 - \beta^2)} a_t^{\beta^2 - 3}.$$

The potential expressed in terms of a is therefore

$$V(a) = \frac{R_1}{2(3 - \beta^2)} a^{-3} [\beta^2 + (6 - \beta^2)F]. \quad (17)$$

where

$$F \equiv (2 - \beta^2)^{-1} \left(\frac{a}{a_t} \right)^{3 - \beta^2}.$$

The remaining physical quantities are

$$H^2 = \frac{R_1}{(3 - \beta^2)} a^{-3} [1 + F] \quad (18)$$

$$\rho_\phi = \frac{R_1}{(3 - \beta^2)} a^{-3} [\beta^2 + 3F] \quad (19)$$

$$p_\phi = -R_1 a^{-3} F \quad (20)$$

$$\omega_\phi = -(3 - \beta^2) \left[\frac{F}{\beta^2 + 3F} \right] \quad (21)$$

$$\Omega_\phi = \frac{1}{3} \left[\frac{\beta^2 + 3F}{1 + F} \right] \quad (22)$$

$$\Omega = \frac{1}{3} \left[\frac{3 - \beta^2}{1 + F} \right] \quad (23)$$

$$q = \frac{1}{2} \left[\frac{1 - (2 - \beta^2)F}{1 + F} \right]. \quad (24)$$

Fixing the present value of one observable quantity determines the others for a given β . For instance, once a_0/a_t is fixed from observation, β may be chosen to reproduce the present values of other parameters. The variation of parameters with β is illustrated in Fig.1.

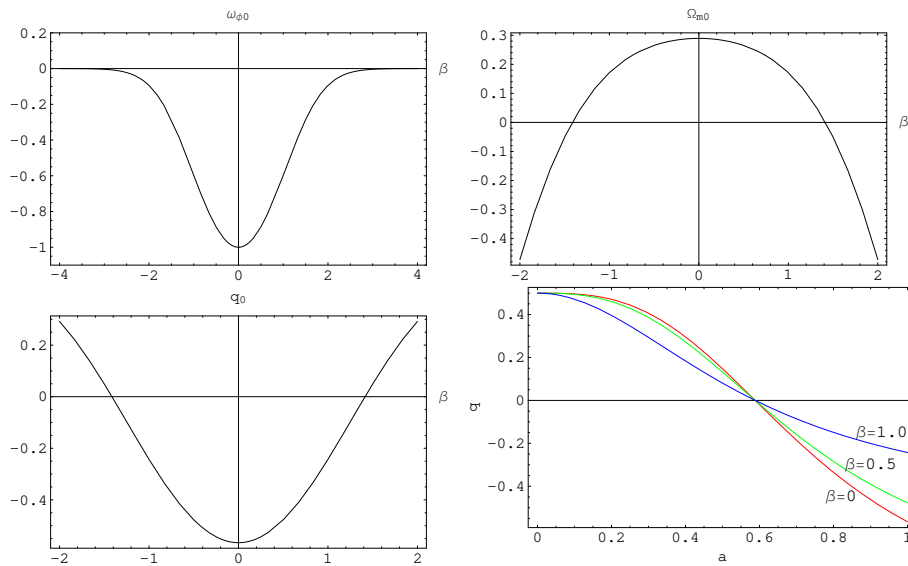


Figure 1: Variation of $\omega_{\phi 0}$, Ω_0 and q_0 with β are shown for $a_0/a_t = 1.7$ in Model 1 along with the nature q vs. a curves for different values β

The plots indicate that present-day observables are only weakly sensitive to β . Given observational uncertainties, the permissible range of β remains relatively broad. Notably, the model reduces to Λ CDM when $\beta = 0$, consistent with expectations that β should be close to zero.

Although Model 1 successfully accounts for late-time acceleration, we now examine whether it can also yield a correct estimate of a_0/a_{eq} once radiation is incorporated.

5 Model 1A

Introducing radiation implies $p \neq 0$. To close the system, we adopt the effective equation of state

$$\omega = \frac{1}{3} \left(1 + \frac{a}{a_{eq}} \right)^{-1}. \quad (25)$$

The conservation equation then gives

$$\rho = R_2 a^{-4} \left(1 + \frac{a}{a_{eq}} \right). \quad (26)$$

Solving the field equations again yields

$$V(a) = \frac{R_2 a^{-4}}{2(3 - \beta^2)} \left[\left(\frac{2}{3} m + \frac{a}{a_{eq}} \right) \beta^2 + (6 - \beta^2) F_1 \right]. \quad (27)$$

where

$$\begin{aligned} m &= \frac{3 - \beta^2}{4 - \beta^2} \\ F_1 &= \left[\frac{8m}{3} \frac{a}{a_t} + \frac{a}{a_{eq}} \right] F. \end{aligned}$$

The other quantities follow as listed below.

$$H^2 = \frac{R_2 a^{-4}}{(3 - \beta^2)} \left[\left(\frac{4}{3} m + \frac{a}{a_{eq}} \right) + F_1 \right] \quad (28)$$

$$\rho_\phi = \frac{R_2 a^{-4}}{(3 - \beta^2)} \left[\left(m + \frac{a}{a_{eq}} \right) \beta^2 + 3F_1 \right] \quad (29)$$

$$p_\phi = R_2 a^{-4} \left[\frac{\beta^2}{3(4 - \beta^2)} - F_1 \right] \quad (30)$$

$$\omega_\phi = \frac{\frac{m}{3} \beta^2 - (3 - \beta^2) F_1}{\left(m + \frac{a}{a_{eq}} \right) \beta^2 + 3F_1} \quad (31)$$

$$\Omega_\phi = \frac{1}{3} \left[\frac{\left(m + \frac{a}{a_{eq}} \right) \beta^2 + 3F_1}{\left(\frac{4}{3} m + \frac{a}{a_{eq}} \right) + F_1} \right] \quad (32)$$

$$\Omega = \frac{1}{3} \left[\frac{\left(1 + \frac{a}{a_{eq}} \right) (3 - \beta^2)}{\left(\frac{4}{3} m + \frac{a}{a_{eq}} \right) + F_1} \right] \quad (33)$$

$$q = \frac{\left(\frac{8m}{3} + \frac{a}{a_{eq}} \right) - (2 - \beta^2) F_1}{\left(\frac{8m}{3} + \frac{2a}{a_{eq}} \right) + 2F_1} \quad (34)$$

Model 1A reduces to Model 1 when $a \gg a_{eq}$ with $R_1 = R_2/a_{eq}$, confirming identical late-time behavior. However, Model 1A now permits estimation of z_{eq} .

To explore parameter dependence, we fix a_0/a_t and Ω_0 . While q_0 and $\omega_{\phi 0}$ remain nearly identical to Model 1, the value of a_0/a_{eq} is extremely sensitive to small changes in β (Fig.2).

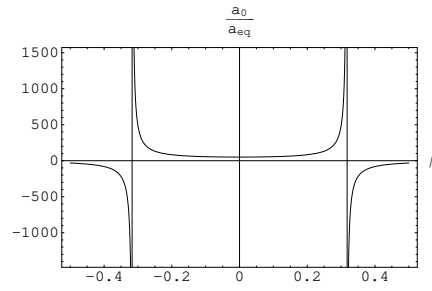


Figure 2: Variation of a_0/a_{eq} with respect to β with $a_0/a_t = 1.7$ and $\Omega_0 = 0.28$ in Model 1A

β	z_{eq}	q_0
0.30000	482.928	-0.534711
0.31000	1203.01	-0.531834
0.31200	1728.83	-0.531247
0.31300	2215.34	-0.530952
0.31400	3086.80	-0.530657
0.31405	3148.84	-0.530642
0.31410	3213.43	-0.530627
0.31420	3350.95	-0.530597
0.31430	3500.81	-0.530568
0.31450	3844.87	-0.530508
0.31500	5099.15	-0.530360

The numerical values shown in the table are computed with $a_0/a_t = 1.7$ and $\Omega_0 = 0.28$. A variation in the third decimal place of β alters a_0/a_{eq} by several hundred. Given the accepted value $z_{eq} = 3196 \pm 134$ [21], β becomes tightly constrained. This makes Model 1A significantly more discriminating than Model 1.

We now investigate whether such sensitivity is a generic feature.

6 Model 2

Here again $\rho = R_3 a^{-3}$, but we assume

$$\dot{\phi} = \alpha a^n. \quad (35)$$

Solving the wave equation gives

$$V(a) = -\frac{\alpha^2}{2} \left(\frac{n+3}{n} \right) a^{2n}. \quad (36)$$

Imposing $q = 0$ at $a = a_t$ yields

$$\alpha^2 = -\frac{R_3}{3} \left(\frac{n}{n+3} \right) a_t^{-(2n+3)}.$$

The potential becomes

$$V(a) = \frac{R_3}{6} (n+3) G a^{-3}. \quad (37)$$

with

$$G = (n + 1)^{-1} \left(\frac{a}{a_t} \right)^{2n+3}.$$

Other quantities are as:

$$H^2 = \frac{R_3}{6} (2 + G) a^{-3} \quad (38)$$

$$\rho_\phi = \frac{R_3}{2} G a^{-3} \quad (39)$$

$$p_\phi = -\frac{R_3}{6} (2n + 3) G a^{-3} \quad (40)$$

$$\omega_\phi = -\frac{1}{3} (2n + 3) \quad (41)$$

$$\Omega_\phi = \frac{G}{2 + G} \quad (42)$$

$$\Omega = \frac{2}{2 + G} \quad (43)$$

$$q = \frac{1 - (n + 1)G}{2 + G} \quad (44)$$

The present value of the parameters are plotted against n by fixing the value of a_0/a_t (Fig.3).

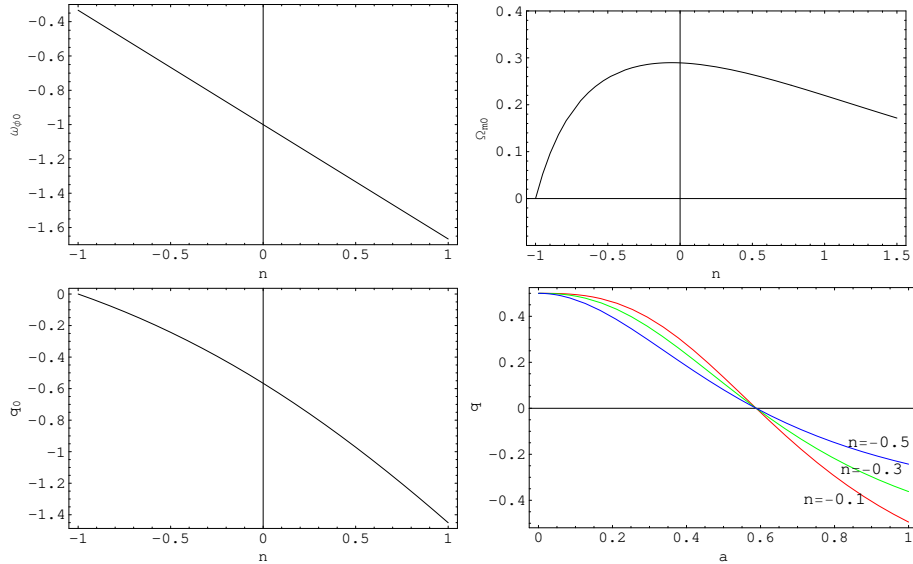


Figure 3: Variation of ω_{ϕ_0} , Ω_0 and q_0 with n are shown for $a_0/a_t = 1.7$ in Model 2 along with the nature of q vs. a curves for different values of n

Analysis show that a small negative n is preferred observationally and also satisfies slow-roll behavior.

7 Model 2A

Radiation is introduced with

$$\omega = \frac{1}{3} \left(1 + \frac{a}{a_{eq}} \right)^{-1}.$$

leading to

$$\rho = R_4 a^{-4} \left(1 + \frac{a}{a_{eq}} \right). \quad (45)$$

The potential becomes

$$V(a) = \frac{R_4}{3} (n+3) G_1 a^{-4}. \quad (46)$$

where

$$G_1 \equiv (n+1)^{-1} \left(1 + \frac{1}{2} \frac{a_t}{a_{eq}} \right) \left(\frac{a}{a_t} \right)^{2n+4}.$$

Other physical quantities are listed below

$$H^2 = \frac{R_4}{3} a^{-4} \left[\left(1 + \frac{a}{a_{eq}} \right) + G_1 \right] \quad (47)$$

$$\rho_\phi = R_4 G_1 a^{-4} \quad (48)$$

$$p_\phi = -\frac{R_4}{3} (2n+3) G_1 a^{-4} \quad (49)$$

$$\omega_\phi = -\frac{1}{3} (2n+3) \quad (50)$$

$$\Omega_\phi = \frac{G_1}{\left(1 + \frac{a}{a_{eq}} \right) + G_1} \quad (51)$$

$$\Omega = \frac{\left(1 + \frac{a}{a_{eq}} \right)}{\left(1 + \frac{a}{a_{eq}} \right) + G_1} \quad (52)$$

$$q = \frac{\left(1 + \frac{1}{2} \frac{a}{a_{eq}} \right) - (n+1) G_1}{\left(1 + \frac{a}{a_{eq}} \right) + G_1} \quad (53)$$

Again, plotting a_0/a_{eq} versus n (Fig.4) shows extreme sensitivity. The values in the table are computed for $a_0/a_t = 1.7$ and $\Omega_0 = 0.28$.

n	z_{eq}	q_0
-0.30000	319.988	-0.363535
-0.31000	654.358	-0.356587
-0.31400	1150.13	-0.353798
-0.31500	1422.49	-0.353102
-0.31720	2991.89	-0.351569
-0.31725	3069.22	-0.351534
-0.31730	3150.67	-0.351500
-0.31740	3327.32	-0.351430
-0.31745	3423.32	-0.351395
-0.31750	3525.05	-0.351360
-0.31800	5017.90	-0.351012

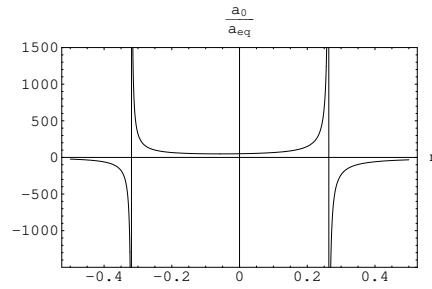


Figure 4: Variation of a_0/a_{eq} with respect to n with $a_0/a_t = 1.7$ and $\Omega_0 = 0.28$ in Model 2A

Thus, the strong dependence of a_0/a_{eq} on model parameters appears to be a generic feature of such scalar field constructions.

8 Conclusion

This work proposes a method to render dark energy models capable of estimating z_{eq} by incorporating an effective radiation–matter equation of state. Two scalar field models (Model 1 and Model 2) were examined, characterized respectively by logarithmic and polynomial evolution of the scalar field. While their late-time behaviors resemble many successful models in the literature, a comparative analysis reveals important distinctions in their physical behavior and observational viability.

Table 1: Comparative analysis of logarithmic and polynomial scalar field models with the standard Λ CDM model:

Logarithmic Model (1/1A)	Polynomial Model (2/2A)	Λ CDM Model
$\phi = \beta \ln a$	$\dot{\phi} \propto a^n$	No scalar field
$V(\phi)$: Exponential-type	Power-law / polynomial-type	Constant Λ
ω_ϕ : evolves with a	$-\frac{1}{3}(2n + 3)$ (constant)	-1 (constant)
q : Smooth transition; tunable via β	Smooth transition; controlled by n	Fixed by Ω_m, Ω_Λ
$\Omega_{\phi 0}, q_0$: Weak sensitivity to β	Weak sensitivity to n	Precisely constrained
z_{eq} : Extremely sensitive to β	Extremely sensitive to n	Robust (~ 3200)
Sensitivity: Very high	Very high	Low
Reduction to Λ CDM: Yes ($\beta = 0$)	No	Fundamental model

The comparative summary presented in Table 1 highlights that, although both scalar field models successfully reproduce late-time cosmological observations, the predicted value of z_{eq} is extremely sensitive to small changes in model parameters constraining their viability. Consequently, observable quantities must be fixed to the third decimal place in order to reproduce the accepted value of z_{eq} .

Therefore, inclusion of the proposed equation of state provides a powerful additional criterion for assessing the viability of dark energy models.

References

- [1] A.G. Riess et al., *Astron. J.* **116**, 1009 (1998); S. Perlmutter et al., *Astrophys. J.* **517**, 565 (1999).
- [2] D.N. Spergel et al., *Astrophys. J. Suppl.* **148**, 175 (2003); D.N. Spergel et al., *Astrophys. J. Suppl.* **170**, 377 (2007); E. Komatsu et al., *Astrophys. J. Suppl.* **180**, 330 (2009).

- [3] D.J. Eisenstein et al., *Astrophys. J.* **633**, 560 (2005); W.J. Percival et al., *Mon. Not. R. Astron. Soc.* **381**, 1053 (2007); W.J. Percival et al., *Mon. Not. R. Astron. Soc.* **401**, 2148 (2010).
- [4] J.C. Carvalho, J.A.S. Lima, I. Waga, *Phys. Rev. D* **46**, 2404 (1992); C. Wetterich, *Astron. Astrophys.* **301**, 321 (1995); A.I. Arbab, *Gen. Relativ. Gravit.* **29**, 61 (1997); T. Padmanabhan, arXiv:gr-qc/0112068; R.G. Vishwakarma, *Class. Quantum Grav.* **19**, 4747 (2002); S.B. Dutta Choudhury, A. Sil, *Astrophys. Space Sci.* **301**, 61 (2006).
- [5] Y. Fujii, *Phys. Rev. D* **26**, 2580 (1982); L.H. Ford, *Phys. Rev. D* **35**, 2339 (1987); C. Wetterich, *Nucl. Phys. B* **302**, 668 (1988); B. Ratra, J. Peebles, *Phys. Rev. D* **37**, 321 (1988); T. Chiba, N. Sugiyama, T. Nakamura, *Mon. Not. R. Astron. Soc.* **289**, L5 (1997); P.G. Ferreira, M. Joyce, *Phys. Rev. Lett.* **79**, 4740 (1997); P.G. Ferreira, M. Joyce, *Phys. Rev. D* **58**, 023503 (1998); R.R. Caldwell, R. Dave, P.J. Steinhardt, *Phys. Rev. Lett.* **80**, 1582 (1998); I. Zlatev, L.M. Wang, P.J. Steinhardt, *Phys. Rev. Lett.* **82**, 896 (1999); P.J. Steinhardt, L.M. Wang, I. Zlatev, *Phys. Rev. D* **59**, 123504 (1999).
- [6] T. Chiba, T. Okabe, M. Yamaguchi, *Phys. Rev. D* **62**, 023511 (2000); C. Armendariz-Picon, V.F. Mukhanov, P.J. Steinhardt, *Phys. Rev. Lett.* **85**, 4438 (2000); C. Armendariz-Picon, V.F. Mukhanov, P.J. Steinhardt, *Phys. Rev. D* **63**, 103510 (2001).
- [7] S.M. Carroll, *Phys. Rev. Lett.* **81**, 3067 (1998); C.F. Kolda, D.H. Lyth, *Phys. Lett. B* **458**, 197 (1999).
- [8] A.Y. Kamenshchik, U. Moschella, V. Pasquier, *Phys. Lett. B* **511**, 265 (2001); M.C. Bento, O. Bertolami, A.A. Sen, *Phys. Rev. D* **66**, 043507 (2002).
- [9] S. Capozziello, *Int. J. Mod. Phys. D* **11**, 483 (2002); S. Capozziello, S. Carloni, A. Troisi, *Recent Res. Dev. Astron. Astrophys.* **1**, 625 (2003); S. Capozziello et al., *Int. J. Mod. Phys. D* **12**, 1969 (2003); S.M. Carroll et al., *Phys. Rev. D* **70**, 043528 (2004); S. Nojiri, S.D. Odintsov, *Phys. Rev. D* **68**, 123512 (2003).
- [10] L. Amendola, *Phys. Rev. D* **60**, 043501 (1999); J.P. Uzan, *Phys. Rev. D* **59**, 123510 (1999); T. Chiba, *Phys. Rev. D* **60**, 083508 (1999); N. Bartolo, M. Pietroni, *Phys. Rev. D* **61**, 023518 (2000); F. Perrotta, C. Baccigalupi, S. Matarrese, *Phys. Rev. D* **61**, 023507 (2000).
- [11] G.R. Dvali, G. Gabadadze, M. Porrati, *Phys. Lett. B* **485**, 208 (2000).
- [12] E.J. Copeland, M. Sami, S. Tsujikawa, *Int. J. Mod. Phys. D* **15**, 1753 (2006); S. Tsujikawa, arXiv:1004.1493 [astro-ph.CO].
- [13] A. Sil, S. Som, *Astrophys. Space Sci.* **318**, 109 (2008).
- [14] G. Zhao et al., *Phys. Lett. B* **648**, 8 (2007).
- [15] A.D. Chernin, *Astron. Zh.* **42**, 1124 (1965); A.D. Chernin, *Nature* **220**, 250 (1968).
- [16] J. McIntosh, *Nature* **215**, 36 (1967); J. McIntosh, *Mon. Not. R. Astron. Soc.* **140**, 461 (1968).
- [17] P.T. Landsberg, D. Park, *Proc. R. Soc. Lond. A* **346**, 485 (1975).
- [18] K.C. Jacobs, *Nature* **215**, 1156 (1967).
- [19] J.M. Cohen, *Nature* **216**, 249 (1967).
- [20] E.J. Copeland, A.R. Liddle, D. Wands, *Phys. Rev. D* **57**, 4686 (1998).
- [21] WMAP Cosmological Parameters, Model LCDM+SZ+LENS, Data WMAP7, NASA LAMBDA, <http://lambda.gsfc.nasa.gov/product/map/dr4/parameters.cfm>.